

# SMALL-SIZE WIRELESS WIDE AREA NETWORK LOOP CHIP ANTENNA FOR CLAMSHELL MOBILE PHONE WITH HEARING-AID COMPATIBILITY

Wei-Yu Li and Kin-Lu Wong

Department of Electrical Engineering, National Sun Yat-Sen University, Kaohsiung 804, Taiwan; Corresponding author: livvy@ema.ee.nsysu.edu.tw

Received 29 January 2009

**ABSTRACT:** A loop chip antenna with an FR4 chip base suitable for clamshell mobile phone application to achieve wireless wide area network operation and hearing-aid compatibility (HAC) is presented. The loop chip antenna is formed by a loop strip excited by a capacitively coupled feed, all printed on the surfaces of the FR4 chip base to achieve a small size of  $1.35 \text{ cm}^3$  only. Two resonant loop paths are provided by the antenna and each loop path can generate its  $0.5\lambda$  and  $1.0\lambda$  resonant modes with good impedance matching. The excited loop resonant modes are formed into two wide operating bands for the antenna to cover GSM850/900 and GSM1800/1900/UMTS operations for both the open (talk) and closed (idle) states of the clamshell mobile phone. Furthermore, the loop antenna also excites small surface currents on the two ground planes of the clamshell mobile phone. In this case, weak near-field EM fields in the vicinity of the mobile phone can be generated. Results show that the strengths of the near-field E-field and H-field fall in the M3 or M4 Category, making the clamshell mobile phone with the proposed antenna to be an HAC communication device. The obtained specific absorption rate values in 1-g and 10-g head tissues also meet the limit of 1.6 and 2.0 W/kg, respectively. © 2009 Wiley Periodicals, Inc. *Microwave Opt Technol Lett* 51: 2327–2335, 2009; Published online in Wiley InterScience (www.interscience.wiley.com). DOI 10.1002/mop.24665

**Key words:** chip antennas; clamshell mobile phone; hearing-aid compatibility; internal mobile phone antennas; loop antennas

## 1. INTRODUCTION

Among various internal mobile phone antennas, the loop antenna has an attractive feature of generating small-excited surface currents on the system ground plane of the mobile phone. This leads to decreasing ground-plane effects on the performances of the internal loop antenna embedded in the mobile phone. This behavior is related to the resonant path being in a closed form for the loop antenna, different from that of the monopoles or planar inverted-F antennas (PIFAs) whose resonant paths are in an open form [1]. In this case, possible coupling between the loop antenna and the system ground plane of the mobile phone will be much smaller than that of the monopoles or PIFAs, thus resulting in decreasing ground-plane effects on the performances of the loop antenna. With this attractive feature, the loop antenna is a very promising candidate for the internal wireless wide area network (WWAN) antenna in the folded-type or clamshell mobile phone [2–9] to achieve good radiation characteristics in both its open (talk) and closed (idle) states, in which the ground-plane conditions varied significantly for the two operating states.

Recently, many promising multiband loop antennas capable of WWAN operation have been reported in the published papers [7, 10–20]. However, most of them are for bar-type mobile phone applications. The promising multiband loop antennas suitable for clamshell mobile phone applications are still very few. In this article, we present a promising small-size loop chip antenna with an FR4 chip base suitable for clamshell mobile phone applications to achieve penta-band WWAN operation in the GSM850/900/

1800/1900/UMTS bands. Note that the proposed loop chip antenna applied in the clamshell mobile phone in its open (talk) and closed (idle) states can all have good impedance matching over the five operating bands, although there are significant ground-plane variations in the two different states. In addition, over the five operating bands, the clamshell mobile phone with the proposed antenna generates weak near-field electric and magnetic fields, allowing it to meet the hearing-aid compatibility (HAC) standard ANSI C63.19-2007 [21], which requires that at least half of all mobile phones on the U.S. market must have RF interference level of at least M3 or M4 Category of the HAC standard [22].

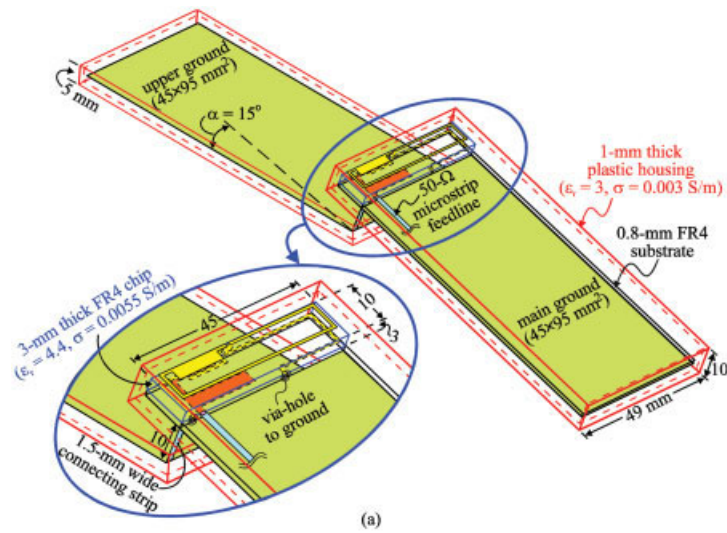
The proposed loop chip antenna in this study is formed by a loop strip excited by a capacitively coupled feed, all printed on the surfaces of the FR4 chip base to achieve a small size of  $45 \times 10 \times 3 \text{ mm}^3$  ( $1.35 \text{ cm}^3$ ) only. The technique of using a capacitively coupled feed has been applied in the loop antenna reported for applications in the bar-type mobile phone [18]. The loop strip of the antenna in Ref. 18 is mounted on the surfaces of the foam base of size  $60 \times 10 \times 3 \text{ mm}^3$  or  $1.8 \text{ cm}^3$ , while the capacitively coupled feed is printed on the system circuit board of the mobile phone. That is, the loop strip and the capacitively coupled feed are not integrated together on the same surface. For practical applications, this may cause fabrication inaccuracy and also inconvenience in obtaining the optimal design dimensions of the antenna. In the proposed antenna, the capacitively coupled feed is also printed on the surface of the FR4 chip base, the same surface as the coupling strip in the loop strip (Fig. 1), which allows good fabrication accuracy to be easily achieved. Furthermore, with the FR4 chip base used, the size of the loop chip antenna is decreased from 1.8 to  $1.35 \text{ cm}^3$  (about 25% in size reduction). A new technique of using a widened section in the loop strip to improve the radiation efficiency of the proposed loop chip antenna over the desired operating bands is also introduced. The specific absorption rate (SAR) results of the proposed antenna in the clamshell mobile phone are also studied.

## 2. DESIGN OF PROPOSED LOOP CHIP ANTENNA

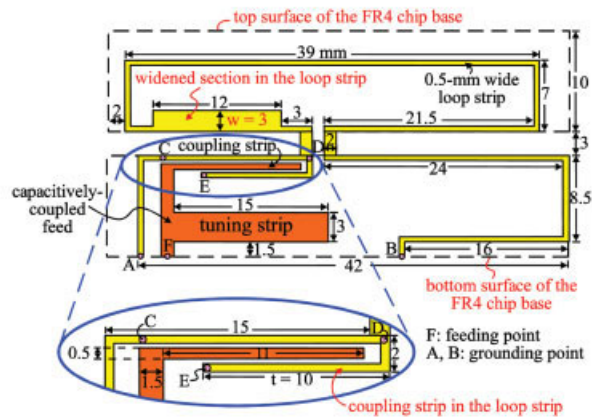
Figure 1(a) shows the geometry of the proposed loop chip antenna for clamshell mobile phone application with HAC. The upper and main ground planes of the clamshell mobile phone are of the same area  $45 \times 95 \text{ mm}^2$  and are connected through a 1.5-mm wide connecting strip of length 10 mm. The main ground plane is printed on the back side of a 0.8-mm thick FR4 substrate of relative permittivity 4.4 and conductivity 0.0055 S/m as the system circuit board of the mobile phone. Notice that there is a top no-ground portion of area  $45 \times 10 \text{ mm}^2$  on the system circuit board, which is used for accommodating the proposed loop chip antenna.

In the study, the inclination angle  $\alpha$  of the upper ground plane (cover) to the axis of the mobile phone is set to  $15^\circ$  for the open (talk) state. While for the closed (idle) state, the angle  $\alpha$  becomes  $180^\circ$ . Also note that the upper and main ground planes are, respectively, enclosed by a 1-mm thick plastic housing of relative permittivity 3.0 and conductivity 0.003 S/m in this study for considering the practical mobile phone housing.

Figure 1(b) shows detailed dimensions of the loop chip antenna in its planar structure. The metal pattern of the antenna is printed on the surfaces of an FR4 chip base with a small volume of  $45 \times 10 \times 3 \text{ mm}^3$  ( $1.35 \text{ cm}^3$  only) and is surface-mounted on the top no-ground position of the main circuit board at the hinge position of the mobile phone. The metal pattern includes a narrow (0.5 mm in width) loop strip excited by a capacitively coupled feed, whose front end (point F) is the antenna's feeding point. For testing the

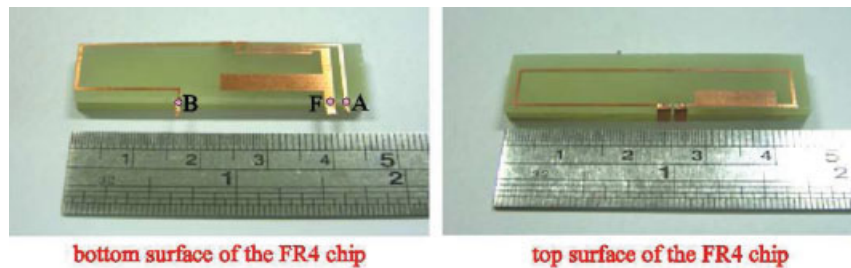


(a)

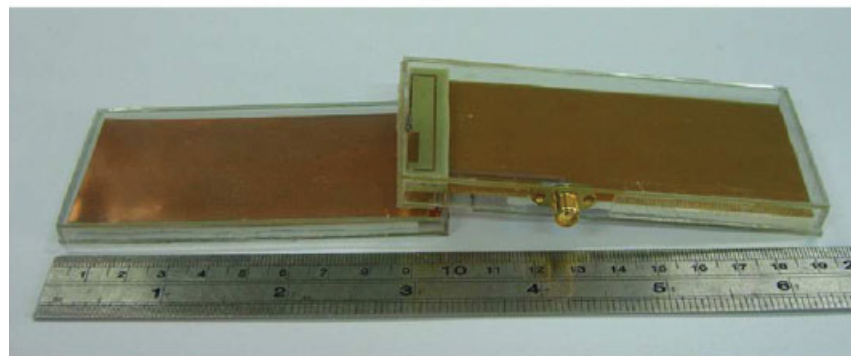


(b)

**Figure 1** (a) Geometry of the proposed WWAN loop chip antenna in the clamshell mobile phone. (b) Dimensions of the loop chip antenna in its planar structure. [Color figure can be viewed in the online issue, which is available at [www.interscience.wiley.com](http://www.interscience.wiley.com)]



(a)



(b)

**Figure 2** Photos of the fabricated prototype. (a) Metal patterns on the top and bottom surfaces of the FR4 chip base. (b) The fabricated antenna with the two ground planes of the clamshell mobile phone. [Color figure can be viewed in the online issue, which is available at [www.interscience.wiley.com](http://www.interscience.wiley.com)]

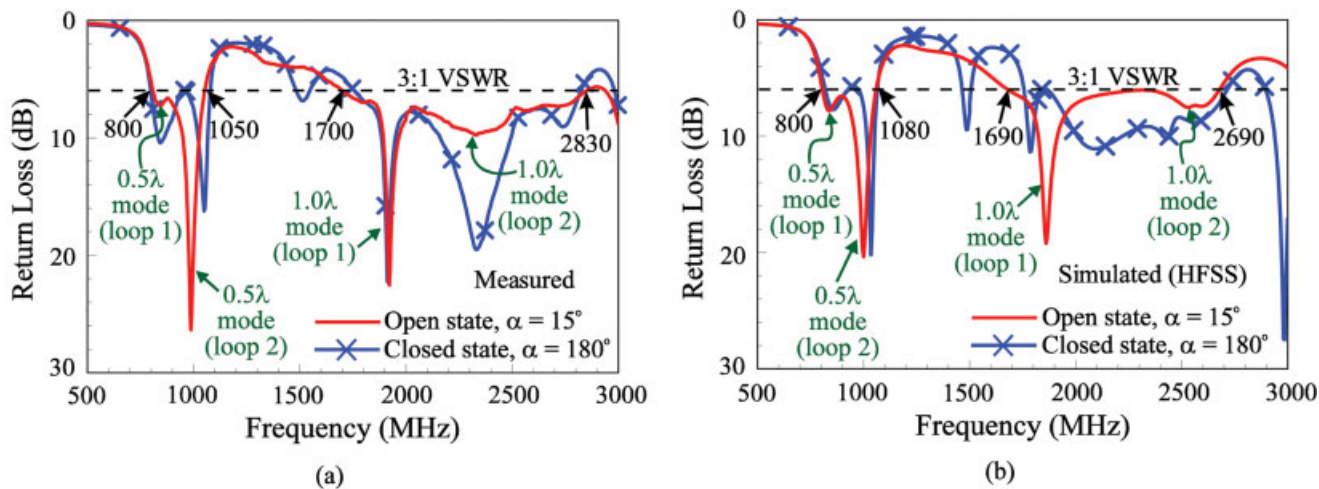


**Figure 3** (a) Measured and (b) simulated return loss of the proposed antenna in the open and closed states of the clamshell mobile phone. [Color figure can be viewed in the online issue, which is available at [www.interscience.wiley.com](http://www.interscience.wiley.com)]

antenna in the experiment, a 50- $\Omega$  microstrip feedline printed on the main circuit board is connected to point F for feeding the antenna. For the loop strip, its two ends (point A and B) are grounded to the top edge of the main ground plane to form a closed loop path.

To integrate the capacitively coupled feed together with the loop strip on the FR4 chip base, an inverted-L coupling strip (section DE) is extended from the loop strip at point D to enhance the energy coupling from the capacitively coupled feed to the loop strip. In the proposed design, two different loop resonant paths are provided. One loop path (Loop 1) starts from point A, through section CD, to point B, whereas the second loop path (Loop 2) is from point F, then through section CD, to point B. The total length of Loop 1 is about 176 mm and its 0.5 $\lambda$  and 1.0 $\lambda$  resonant modes are excited at about 0.85 and 1.9 GHz in this study. For Loop 2, its length is about 162 mm and its 0.5 $\lambda$  and 1.0 $\lambda$  resonant modes are excited at about 1.0 and 2.2 GHz. The successful excitation of the four resonant modes contributed by Loop 1 and 2 is owing to the use of the capacitively coupled feed printed on the same surface as the loop strip. With the four resonant modes excited, two wide operating bands for the antenna's lower and upper bands to easily

cover GSM850/900 and GSM1800/1900/UMTS operations in both the open and closed states of the clamshell mobile phone are obtained.

Also note that in comparison to the case of using a foam base (relative permittivity close to 1.0) in Ref. 18, the required length of the loop strip is reduced by 89 mm, mainly because of the material effect of the FR4 chip base. The decrease in the required length of the loop strip also leads to the simplified structure of the proposed antenna, compared with that in Ref. 18, and results in a more compact size. In addition, a widened section of length 12 mm and width ( $w$ ) 3 mm is introduced in the loop strip near point D. By selecting the widened section properly, good radiation efficiency of the proposed antenna over the upper band for GSM1800/1900/UMTS operation can be achieved. For the function of the tuning strip of the capacitively coupled feed, it is used for adjusting the impedance matching of the antenna's upper band, similar as that in Ref. 18.

### 3. RESULTS AND DISCUSSION

The proposed loop chip antenna was fabricated and tested. The photos of the fabricated prototype are shown in Figure 2. Figure

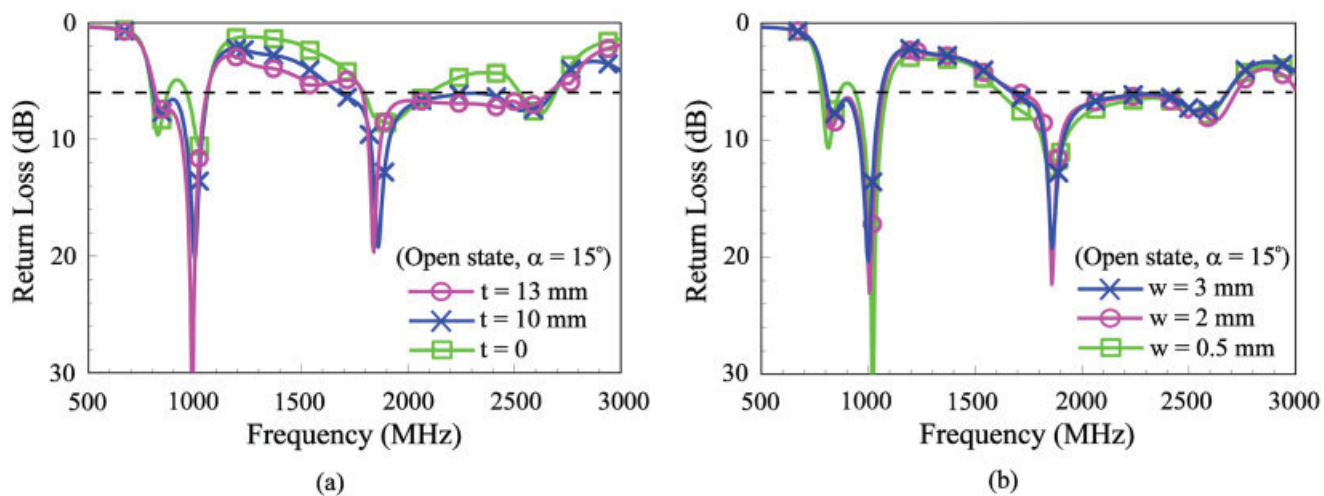


**Figure 4** Simulated return loss as a function of (a) the length  $t$  of the coupling strip and (b) the width  $w$  of the widened section in the loop strip. Other dimensions are the same as given in Figure 1. [Color figure can be viewed in the online issue, which is available at [www.interscience.wiley.com](http://www.interscience.wiley.com)]

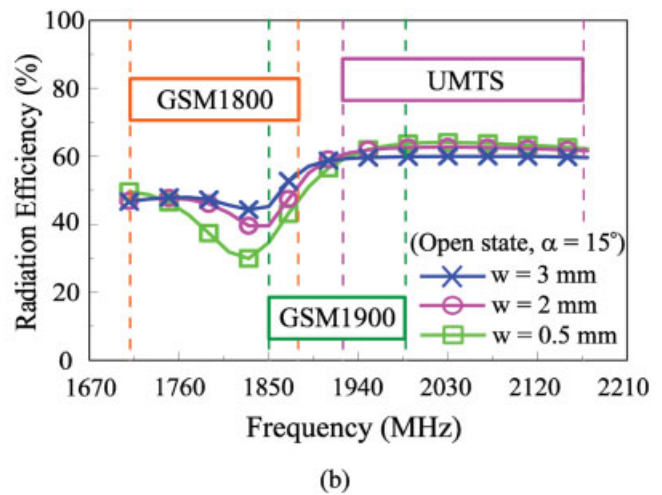
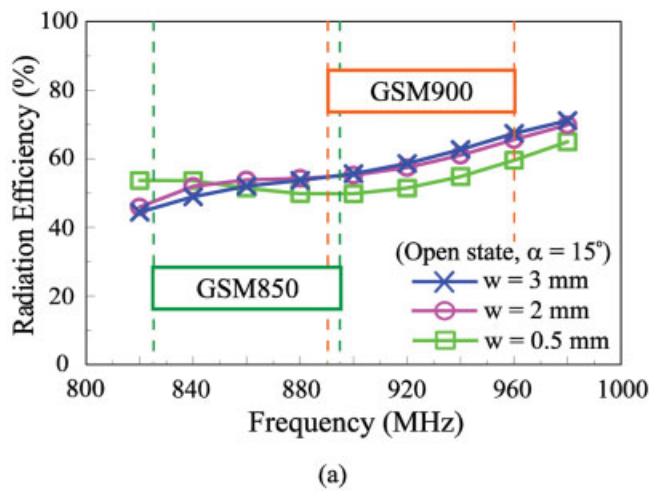


**Figure 5** Simulated radiation efficiency as a function of the width  $w$  of the widened section in the loop strip. Other dimensions are the same as given in Figure 1. (a) The GSM850/900 bands. (b) The GSM1800/1900/UMTS bands. [Color figure can be viewed in the online issue, which is available at [www.interscience.wiley.com](http://www.interscience.wiley.com)]

3(a) shows the measured return loss of the constructed prototype in the open and closed states of the clamshell mobile phone. The corresponding simulated results obtained using Ansoft HFSS [23] are shown in Figure 3(b). From the results shown in Figures 3(a) and 3(b), good agreement between the measurement and simulation is seen. Also, as seen in Figure 3(a) for the measured results in the open state, the antenna's lower band at about 900 MHz is formed by two resonant modes, which are the  $0.5\lambda$  resonant modes of Loop 1 and 2 as discussed in section 2. The impedance bandwidth defined by 3:1 VSWR (6-dB return loss, a widely used value for internal mobile phone antennas) reaches 250 MHz (800–1050 MHz) and easily covers GSM850/900 operation. For the antenna's upper band, it is also mainly formed by two resonant modes, which are two  $1.0\lambda$  resonant modes of Loop 1 and 2. The obtained impedance bandwidth is as large as 1130 MHz (1700–2830 MHz) and easily covers GSM1800/1900/UMTS operation. In addition, in the closed state of the clamshell mobile phone, the obtained 3:1 VSWR bandwidth can still be large enough for the antenna to cover the desired five operating bands for WWAN operation.

Effects of the coupling strip in the loop strip are studied in Figure 4(a), in which the simulated return loss for the length  $t$  of the coupling strip varied from 0 to 13 mm is shown. Results indicate that when the coupling strip is not present ( $t = 0$ ), good impedance matching of the frequencies over the antenna's lower and upper bands cannot be obtained. With the presence of the coupling strip, especially for a longer length of  $t = 13$  mm, enhanced impedance matching over the antenna's lower and upper bands is obtained.

Effects of the widened section in the loop strip are also analyzed. Results of the simulated return loss for the width  $w$  of the widened section varied from 0.5 to 3 mm are presented in Figure 4(b). Small variations in the impedance matching over the antenna's lower and upper bands are seen. However, the radiation efficiency of the antenna over the GSM1800 band can be greatly improved by increasing the width  $w$  of the widened section. Figures 5(a) and 5(b) show the simulated radiation efficiency over the lower and upper bands as a function of the width  $w$ . For the width  $w$  varied from 0.5 to 3 mm, stable radiation efficiency acceptable for practical applications is seen over the lower band shown in Figure 5(a). However, only when the width  $w$  is increased to be 3 mm, the radiation efficiency over the GSM1800

band of the antenna can be greatly improved to acceptable levels for practical applications. This is largely because the widened section in the loop strip can result in stronger excited surface currents for frequencies over the GSM1800 band, which leads to increased radiation efficiency for the antenna.

The simulated excited surface current distributions on the upper and main ground planes of the clamshell mobile phone at 925, 1795, and 2045 MHz are shown in Figure 6. Small surface currents

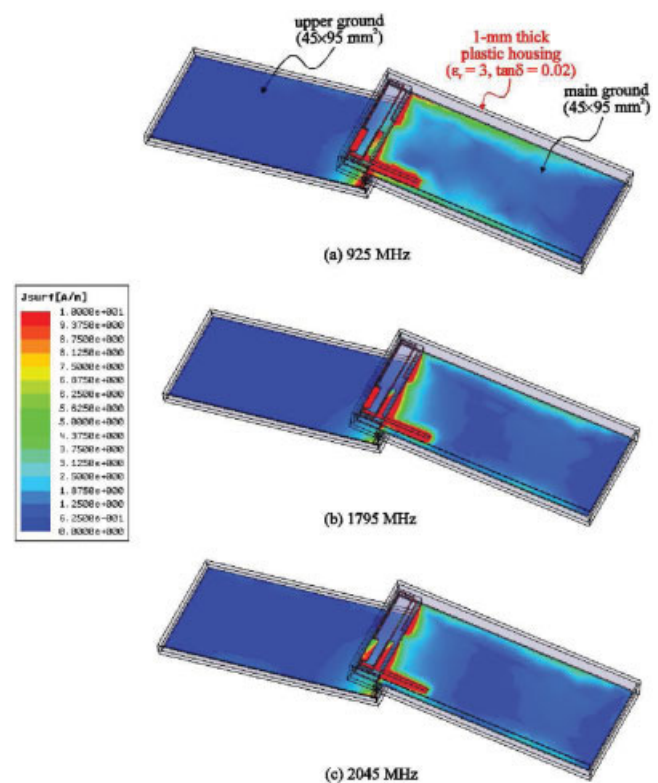


**Figure 6** Simulated surface current distributions on the proposed antenna and the two ground planes. (a) 925 MHz. (b) 1795 MHz. (c) 2045 MHz. [Color figure can be viewed in the online issue, which is available at [www.interscience.wiley.com](http://www.interscience.wiley.com)]

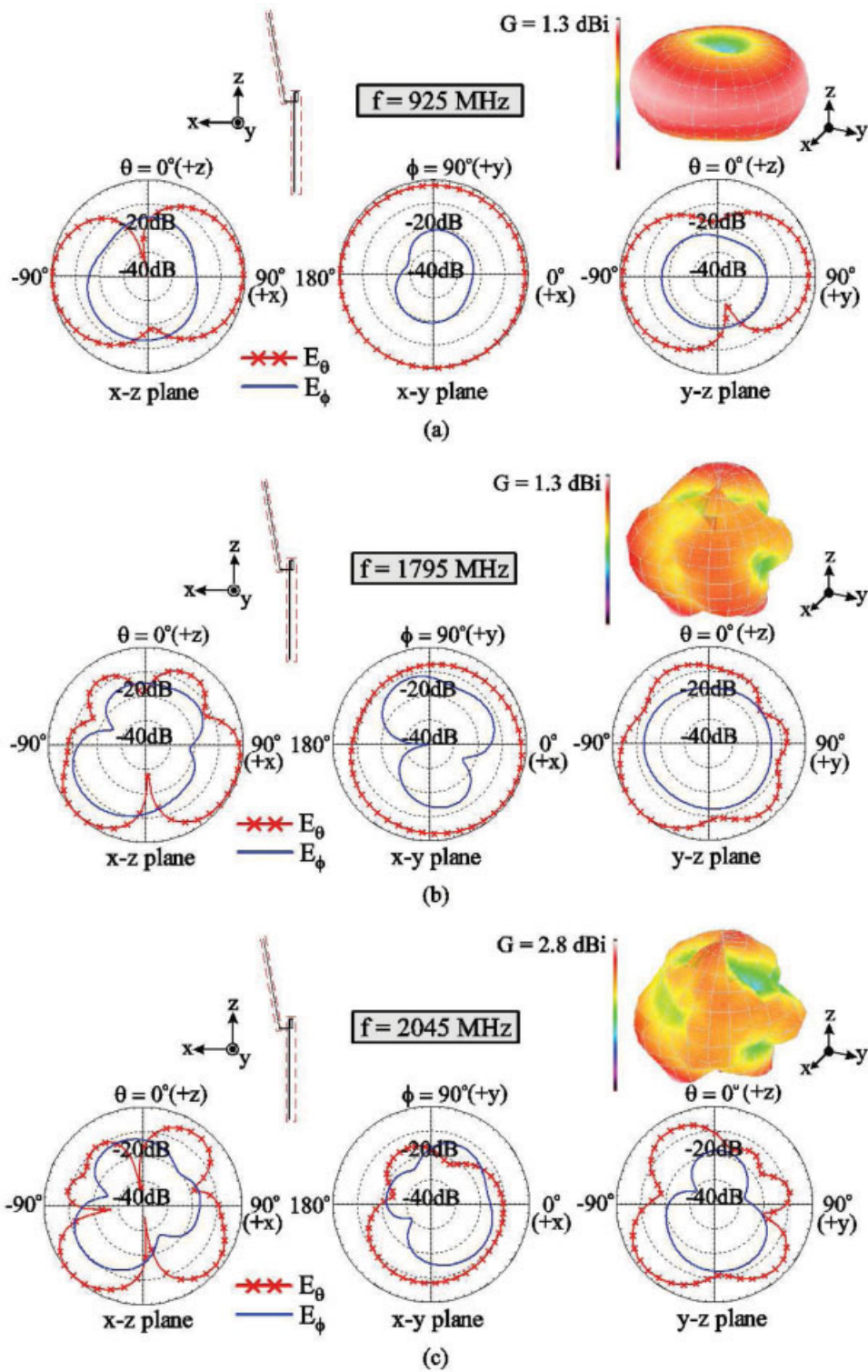


**Figure 7** Measured 3-D and 2-D radiation patterns for the proposed antenna in the open state. (a) 925 MHz. (b) 1795 MHz. (c) 2045 MHz. [Color figure can be viewed in the online issue, which is available at [www.interscience.wiley.com](http://www.interscience.wiley.com)]

are excited on the two ground planes of the mobile phone, especially on the upper ground plane. This behavior can result in small near-field electric and magnetic fields of the mobile phone. It is also seen that owing to the  $1.0\lambda$  resonant mode being the balanced mode of the loop antenna, the strength of the excited surface currents on the main ground plane at 1795 and 2045 MHz are smaller than those at 925 MHz.

Radiation characteristics of the constructed prototype in the open state of the clamshell mobile phone are studied in Figures 7 and 8. The measured three-dimensional (3-D) and two-dimensional (2-D) radiation patterns at 925, 1795, and 2045 MHz are plotted in Figure 7. At 925 MHz, dipole-like radiation patterns are seen. While at 1795 and 2045 MHz, more variations in the radiation patterns are seen, which is expected for the antenna operated

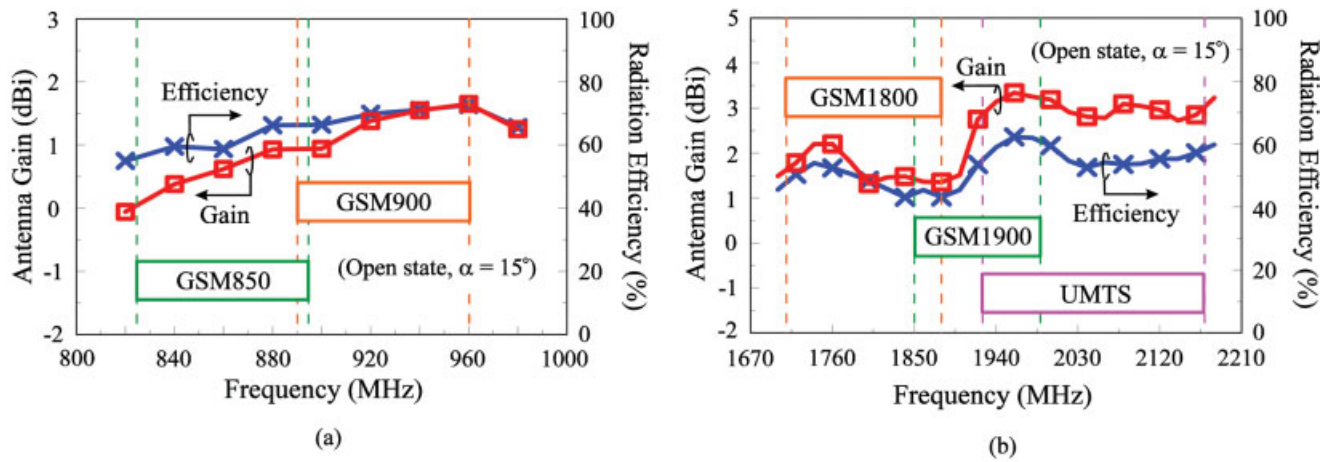


**Figure 8** Measured radiation efficiency and antenna gain for the proposed antenna in the open state. (a) The GSM850/900 bands. (b) The GSM1800/1900/UMTS bands. [Color figure can be viewed in the online issue, which is available at [www.interscience.wiley.com](http://www.interscience.wiley.com)]

at its upper band. The measured radiation efficiency and antenna gain are presented in Figure 8. Over the GSM850/900 bands shown in Figure 8(a), the radiation efficiency is all better than 50%, and the antenna gain is about 0.1–1.7 dBi. Figure 8(b) shows the results over the GSM1800/1900/UMTS bands. The radiation efficiency is about 45–60%, and the antenna gain is about 1.5–3.3 dBi. The obtained radiation characteristics are generally acceptable for practical mobile phone applications.

For the HAC and SAR studies of the proposed antenna, the simulated results obtained using SEMCAD simulation software

[24] are analyzed. Figure 9 shows the HAC simulation model of the clamshell mobile phone with the proposed antenna. Based on the HAC standard ANSI C63.19-2007 [21], the observation plane for the near-field electric and magnetic fields is centered above the acoustic output center with an area of  $50 \times 50 \text{ mm}^2$  and a distance of 15 mm. The observation plane is further divided into nine equal cells. Table 1 lists the results of the peak E-field and H-field strengths among the nine cells (excluding three consecutive cells along the boundary of the observation plane that have the strongest field strengths [21], see Fig. 10) at the central frequencies of the

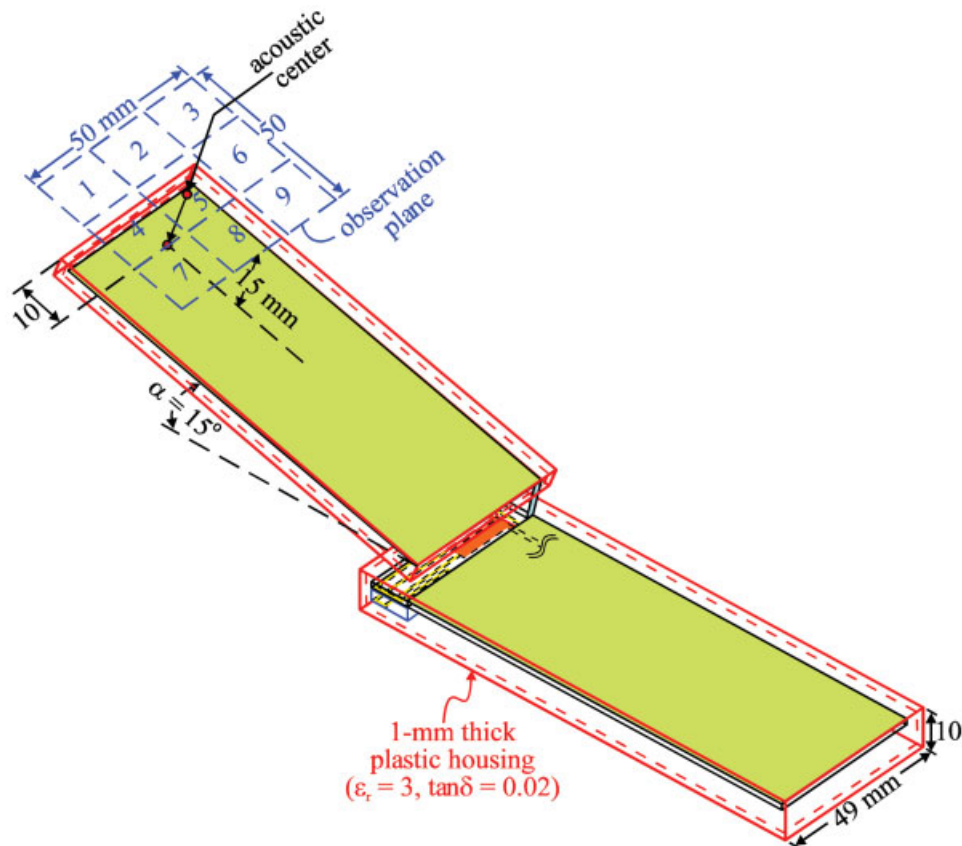


**Figure 9** HAC simulation model provided by SEMCAD [24] complying with the standard ANSI C63.19-2007 [21]. [Color figure can be viewed in the online issue, which is available at [www.interscience.wiley.com](http://www.interscience.wiley.com)]

**TABLE 1 Simulated Peak Value of the E-Field and H-Field Strengths on the Observation Plane of the HAC Simulation Model in Figure 9**

Frequency (MHz)	859	925	1795	1920	2045
E-field (V/m)	122 (41.7 dB)	144 (43.2 dB)	67.8 (36.6 dB)	63.4 (36.0 dB)	22.4 (27.0 dB)
E-field Category	M4	M4	M3	M3	M4
H-field (A/m)	0.22 (-13.2 dB)	0.26 (-11.7 dB)	0.2 (-14.0 dB)	0.22 (-13.2 dB)	0.08 (-21.9 dB)
H-field Category	M4	M4	M3	M3	M4

five operating bands. Also note that for the GSM850/900 bands, the testing power is 33 dBm (2 W continuous wave power). For the GSM1800/1900 bands and the UMTS band, the testing power is 30 dBm (1 W continuous wave power) and 21 dBm (0.125 W continuous wave power), respectively. From the obtained HAC results, the generated near-field strengths of the proposed antenna are evaluated and rated to be in the M3 or M4 Category meeting the standard ANSI C63.19-2007 [21]. The simulated near-field E-field and H-field strength distributions on the observation plane and the peak E-field and H-field strengths in the nine cells at 925, 1795, and 2045 MHz are also presented in Figure 10 for comparison.

The SAR simulation model (SEMCAD [24]) for the clamshell mobile phone with the proposed antenna is shown in Figure 11(a). The plastic housing of the upper ground plane of the mobile phone is attached onto the right phantom cheek, and the position of the acoustic center of the mobile phone is close to the phantom ear. The phantom head model consists of a thin head shell and head liquid, whose parameters for the GSM850/900 bands and the GSM1800/1900/UMTS bands are listed in Table 2. The simulated SAR distributions on the phantom head at 925, 1795, and 2045 MHz are shown in Figure 11(b).

From the SAR distributions, it is seen that the position of the local SAR maximum on the phantom head at lower and upper

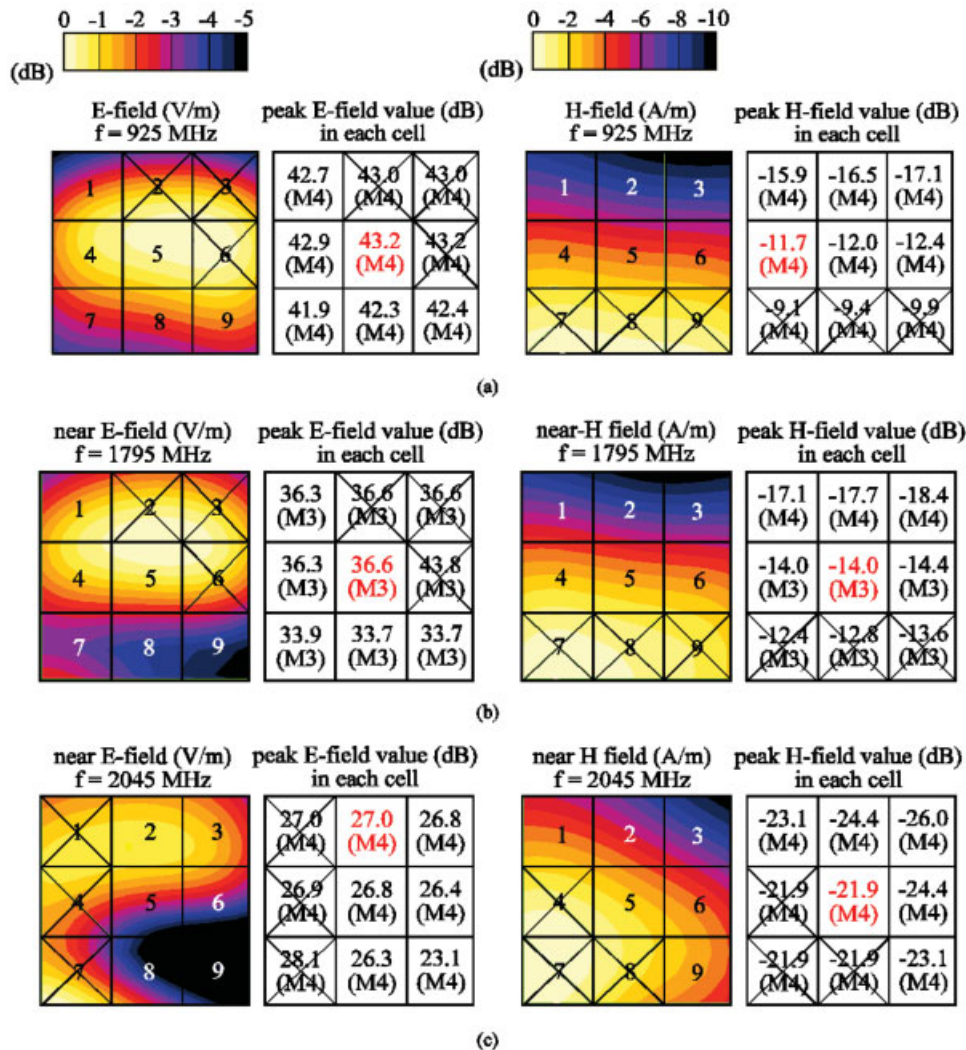


**Figure 10** Simulated E-field and H-field strength distributions and their peak values in each cell of the observation plane shown in Figure 9. (a) 925 MHz. (b) 1795 MHz. (c) 2045 MHz. [Color figure can be viewed in the online issue, which is available at [www.interscience.wiley.com](http://www.interscience.wiley.com)]

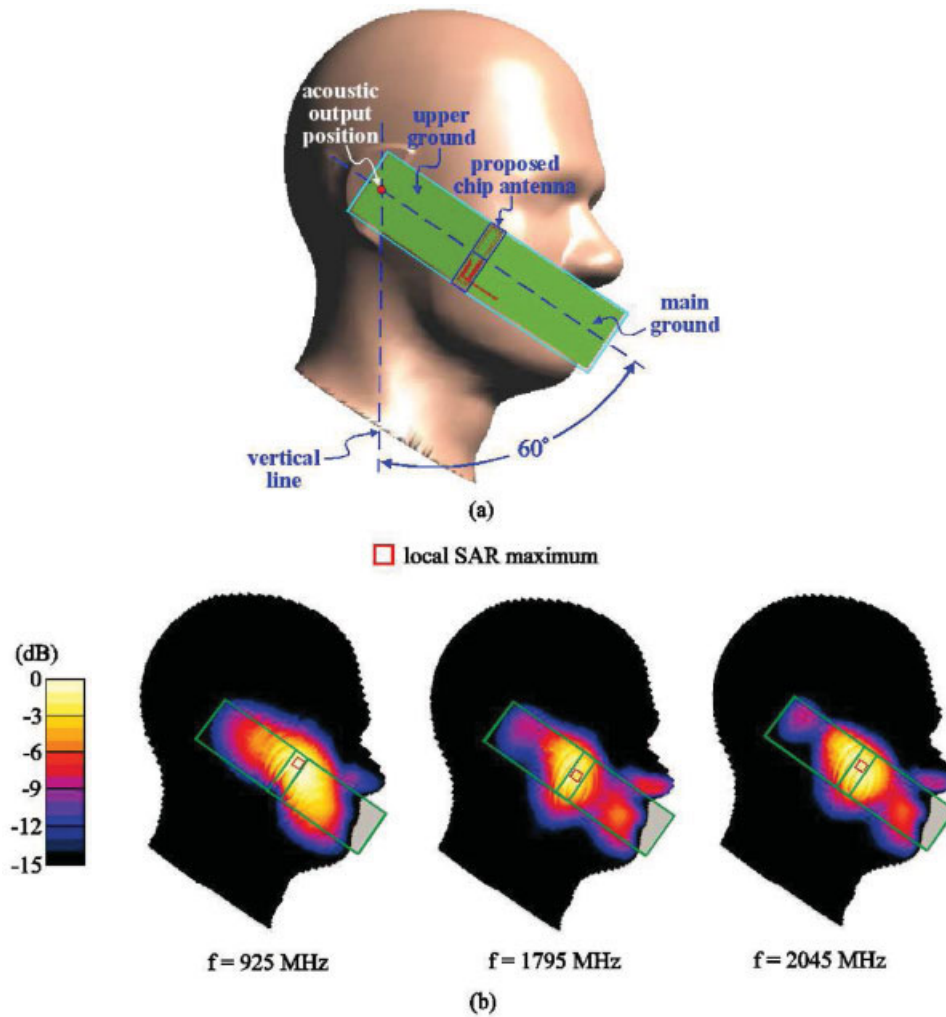


**Figure 11** (a) SAR simulation model provided by SEMCAD [24] with the upper plastic housing (cover) of the clamshell mobile phone attached onto the right phantom cheek. (b) Simulated SAR distributions on the phantom head at 925, 1795, and 2045 MHz. [Color figure can be viewed in the online issue, which is available at [www.interscience.wiley.com](http://www.interscience.wiley.com)]

frequencies are all located at about the hinge position of the mobile phone. The SAR distributions on the phantom head become weaker toward the top edge of the upper ground plane. The results suggest that the SAR contributed from the excited surface currents on the upper ground plane by the proposed loop antenna is small. Table 3 lists the simulated SAR results for the 1-g and 10-g head tissues at the central frequencies of the five operating bands. For the GSM850/900 and GSM1800/1900/UMTS bands, the SAR is tested using 24 dBm (1/8 of the 2 W continuous wave power) and 21 dBm (1/8 of the 1 W continuous wave power for GSM1800/1900 systems and 0.125 W continuous wave power for UMTS system) [17], respectively.

**TABLE 2** Parameters of the SAR Simulation Phantom Head Shown in Figure 11(a)

	GSM850/900 Bands		GSM1800/1900/UMTS Bands	
	$\epsilon_r$	$\sigma$ (S/m)	$\epsilon_r$	$\sigma$ (S/m)
Head liquid	41.5	0.97	40	1.4
Head shell	3.5	0	3.5	0

The obtained 1-g and 10-g SAR values are seen to easily meet the limit of 1.6 and 2.0 W/kg, respectively.

#### 4. CONCLUSIONS

A small-size loop chip antenna suitable for covering GSM850/900/1800/1900/UMTS operations in the hearing-aid compatible clamshell mobile phone has been proposed. The antenna is fabricated on a small FR4 chip base of size 1.35 cm<sup>3</sup> and is easy to fabricate at low cost. Good radiation characteristics for frequencies over the five operating bands have been obtained. Furthermore, owing to the loop metal pattern used for the antenna, the excited surface currents on the two ground planes of the clamshell mobile phone, especially the upper ground plane, are small. This behavior makes the obtained operating bandwidths of the antenna for the clamshell mobile phone in the open and closed states about the same,

**TABLE 3** Simulated SAR Values for the Simulation Model Shown in Figure 11(a)

Frequency (MHz)	859	925	1795	1920	2045
1-g SAR (W/kg)	0.71	0.88	0.42	0.55	0.52
10-g SAR (W/kg)	0.50	0.61	0.28	0.36	0.35

although the ground-plane conditions are greatly different for the two different operating states. This behavior also leads to small HAC and SAR values obtained for the proposed antenna for the clamshell mobile phone applications.

## REFERENCES

1. K.L. Wong, Planar antennas for wireless communications, Wiley, New York, 2003.
2. T. Sugiyama, H. Horita, Y. Shirakawa, M. Ikegaya, S. Takaba, and H. Tate, Triple-band internal antenna for clamshell type mobile phone, Hitachi cable review, Hitachi Co., Japan 2003, pp. 26–31.
3. K.L. Wong, S.W. Su, C.L. Tang, and S.H. Yeh, Internal shorted patch antenna for a UMTS folder-type mobile phone, IEEE Trans Antennas Propag 53 (2005), 3391–3394.
4. K.L. Wong, W.C. Su, and F.S. Chang, Wideband internal folded planar monopole antenna for UMTS/WiMAX folder-type mobile phone, Microwave Opt Technol Lett 48 (2006), 324–327.
5. K.L. Wong, Y.W. Chi, B. Chen, and S. Yang, Internal DTV antenna for folder-type mobile phone, Microwave Opt Technol Lett 48 (2006), 1015–1019.
6. B.S. Collins, Improving the RF performance of clamshell handsets, IEEE International Workshop on Antennas Technology Small Antenna and Novel Metamaterials, 2006, pp. 265–268.
7. K.L. Wong and S.Y. Tu, Ultra-wideband loop antenna coupled-fed by a monopole feed for penta-band folder-type mobile phone, Microwave Opt Technol Lett 50 (2008), 2706–2712.
8. C.I. Lin and K.L. Wong, Printed monopole slot antenna for penta-band operation in the folded-type mobile phone, Microwave Opt Technol Lett 50 (2008), 2237–2242.
9. C.H. Chang, K.L. Wong, and J.S. Row, Coupled-fed small-size PIFA for penta-band folder-type mobile phone application, Microwave Opt Technol Lett 51 (2009), 18–23.
10. B.K. Yu, B. Jung, H.J. Lee, F.J. Harackiewicz, and B. Lee, A folded and bent internal loop antenna for GSM/DCS/PCS operation of mobile handset applications, Microwave Opt Technol Lett 48 (2006), 463–467.
11. B. Jung, H. Rhyu, Y.J. Lee, F.J. Harackiewicz, M.J. Park, and B. Lee, Internal folded loop antenna with tuning notches for GSM/GPS/DCS/PCS mobile handset applications, Microwave Opt Technol Lett 48 (2006), 1501–1504.
12. W.Y. Li and K.L. Wong, Internal printed loop-type mobile phone antenna for penta-band operation, Microwave Opt Technol Lett 49 (2007), 2595–2599.
13. W.Y. Li and K.L. Wong, Surface-mount loop antenna for AMPS/GSM/DCS/PCS operation in the PDA phone, Microwave Opt Technol Lett 49 (2007), 2250–2254.
14. Y.W. Chi and K.L. Wong, Internal compact dual-band printed loop antenna for mobile phone application, IEEE Trans Antennas Propag 55 (2007), 1457–1462.
15. C.I. Lin and K.L. Wong, Internal meandered loop antenna for GSM/DCS/PCS multiband operation in a mobile phone with the user's hand, Microwave Opt Technol Lett 49 (2007), 759–765.
16. K.L. Wong and C.H. Huang, Printed loop antenna with a perpendicular feed for penta-band mobile phone application, IEEE Trans Antennas Propag 56 (2008), 2138–2141.
17. Y.W. Chi and K.L. Wong, Compact multiband folded loop chip antenna for small-size mobile phone, IEEE Trans Antennas Propag 56 (2008), 3797–3803.
18. W.Y. Li and K.L. Wong, Seven-band surface-mount loop antenna with a capacitively coupled feed for mobile phone application, Microwave Opt Technol Lett 51 (2009), 81–88.
19. Y.W. Chi and K.L. Wong, Very-small-size printed loop antenna for GSM/DCS/PCS/UMTS operation in the mobile phone, Microwave Opt Technol Lett 51 (2009), 184–192.
20. M.R. Hsu and K.L. Wong, Seven-band folded-loop chip antenna for WWAN/WLAN/WiMAX operation in the mobile phone, Microwave Opt Technol Lett 51 (2009), 543–549.
21. American National Standards Institute, American National Standard for Method of Measurement of Compatibility between Wireless com-

munication Devices and Hearing Aids (ANSI C63.19-2007), American National Standards Institute, New York, 2007.

22. T. Yang, W.A. Davis, W.L. Stutzman, and M.C. Huynh, Cellular-phone and hearing-aid interaction: An antenna solution, IEEE Antennas Propag Mag 50 (2008), 51–65.
23. Available at: <http://www.ansoft.com/products/hf/hfss/>, Ansoft Corporation HFSS.
24. Available at: <http://www.semcad.com>, SEMCAD, Schmid & Partner Engineering AG (SPEAG).

© 2009 Wiley Periodicals, Inc.

## SECOND-ORDER STATISTICS OF MEASURED ON-BODY DIVERSITY CHANNELS

Imdad Khan, Y. I. Nechayev, and Peter S. Hall

Department of EECE, University of Birmingham, Edgbaston, Birmingham, United Kingdom; Corresponding author: imdadkhalil@yahoo.com

Received 29 January 2009

**ABSTRACT:** *The fading severity, and the improvement offered by diversity to reduce it, is presented in the context of the second-order statistics for on-body belt-head channel. Average LCR and AFD values are presented and compared at three frequencies and also for the three antennas for branch and combined signals.* © 2009 Wiley Periodicals, Inc. Microwave Opt Technol Lett 51: 2335–2337, 2009; Published online in Wiley InterScience (www.interscience.wiley.com). DOI 10.1002/mop.24621

**Key words:** *fading channels; diversity; level crossing rate; average fade duration; on-body channels*

### 1. INTRODUCTION

Body-centric wireless communication is an important branch of personal communication systems. The ever increasing use of wireless devices in personal healthcare, entertainment, security and personal identification, fashion, and personalized communications, etc., drives research to establish more reliable and efficient link between the devices mounted on the body. The high data rate and reliable transmission between the body-worn wireless devices demand the use of multiple antennas. Antenna diversity is a well known technique to overcome fading and provide a power efficient link, where two or more signals from various uncorrelated diversity branches are combined in different ways to achieve the diversity combined signal. The use of diversity removes the deep fades and, as a result, the rate of crossing and the duration of the lower fade levels are reduced for the resultant combined signal. The amount of improvement offered by diversity is quantified by the diversity gain but can also be estimated from the second-order statistics.

The fading in the on-body channels is mainly caused by the movement of the scatterers surrounding the antennas. Most of the work so far, on the on-body channels, characterizes the antennas and estimation of the first-order statistics [1–3]. The diversity performance analysis at various frequencies has also been investigated [4–6]. Recently, the characterization of the on-body diversity channels has been reported in [7]. The estimation and comparison of the second-order statistics of branch and diversity combined signal has been done extensively for the mobile indoor scenarios [8–10], but has not been attempted so far for on-body channels to the best of our knowledge.